

Cong-Nam Tran*, Nam-Hoang Nguyen* and Trong-Minh Hoang

Lightbeam Configuration Method and Interference Elimination Resource Scheduling for Indoor Multibeam VLC Networks

<https://doi.org/10.1515/joc-2018-0224>

Received December 10, 2018; accepted February 02, 2019

Abstract: Visible light communications (VLC) is considered as an alternative communications technology for providing indoor wireless services. VLC systems are expected to offer high data transmission rate and seamless coverage. In order to achieve these requirements, VLC systems utilizing multi-lightbeam access points (multi-beam VLC-AP) for downlink transmission have been proposed recently. In this paper, we present a lightbeam configuration method and an interference elimination resource scheduling mechanism (IERS) for indoor multi-beam multi-access point VLC systems. The proposed lightbeam configuration method ensures seamless connectivity between user equipment and VLC-AP. The proposed IERS mechanism consists of a beam assignment algorithm and a resource allocation algorithm for eliminating co-channel interference as well as improving system performance. Performance results obtained by computer simulation indicate that there are significant improvements in terms of downlink signal to interference plus noise ratio, user throughput and packet delay when the proposed IERS mechanism is deployed.

Keywords: visible light communications, indoor multi-beam VLC, resource scheduling, co-channel interference

1 Introduction

The exponential growth of wireless traffic demand results in a congested, scarce and expensive RF spectrum, limiting the achievable capacity of wireless networks [1]. To overcome this limitation, Visible Light Communications (VLC) using low power Light Emitting Diode (LED) to provide not only lighting but also data transmission is considered as a

promising indoor communications technology for next generation broadband communications [2]. VLC has many advantages including high license free spectrum bandwidth (from 400 THz to 800 THz, high area spectral performance, dual functions (lighting and data transmission), energy efficiency and high security [3–5].

Indoor VLC systems must ensure efficient illumination over entire area of the room and the seamless communications between user equipments (UEs) and VLC access points (VLC-Aps) (for short, called as APs). In addition, indoor VLC systems need to achieve high data rate to meet the increasing demand of users. In order to enhance the signal quality and support high user density, indoor VLC systems using multi-beam APs have been proposed recently [6–8]. However, there are existing technical challenges which have not been solved in recent papers. VLC systems in [6] achieve low spectral efficiency since there are large overlapped areas among neighbor APs resulting in high co-channel interference (CCI). Additionally, VLC systems described in [7] are not able so support high user density because they deploy only one lightbeam (for short, called as beam) serves a single UE in a time slot. This limitation is solved by using optical beamforming Space Division Multiple Access (SDMA) in [8] in which more UEs can get data transmission at the same time. In order to exploit multi-beam (beamforming) VLC systems, beam configuration is an important task and some configuration methods have been proposed recently. For example, signal to interference plus noise ratio (SINR) with AP configurations has been analyzed in [9, 10]. Moreover, the deployment of multi-element angle diversity transmitters in VLC systems has been proposed in [9, 11] where each beam is controlled by an electronic element of the multi-element transmitter. Performance analysis shown in [11] demonstrates that using multibeam VLC-APs is able to provide high area spectrum efficiency. Deploying multibeam VLC-APs proved to be a scheme that supports high security at the physical layer [12].

In multibeam VLC systems using the optical SDMA, there are intra-cell and inter-cell CCI which decrease SINR of UEs residing in overlapping regions [11]. Minimizing intra-cell and inter-cell CCI is an important task, particularly for dense VLC-AP deployment scenarios. We can find

*Corresponding authors: Cong-Nam Tran, trancongnam14@gmail.com and Nam-Hoang Nguyen, hoangnn@vnu.edu.vn, University of Engineering and Technology, Vietnam National University, Hanoi, Vietnam

Trong-Minh Hoang, Posts and Telecommunications Institute of Technology, Hanoi, Viet Nam, E-mail: hoangtrongminh@ptit.edu.vn

several approaches to reducing CCI in optical wireless systems proposed recently. Applying static resource partitioning was used in [13] to avoid CCI in cellular optical wireless systems. Using different wavelengths in [14] to avoid CCI in femtocell VLC systems. However, the spectral efficiency is decreased in these two studies. In [15], two fractional frequency reuse schemes called strict fractional frequency reuse and soft frequency reuse was proposed. Simulation results showed that SINR of cell-edge UEs and spectral efficiency were improved when compare with those of the full frequency reuse scheme. Still using fractional frequency reuse did not utilize full frequency resource. Reducing CCI effects can be carried out at the physical layer. A self-organizing interference coordination technique based on the busy-burst signaling was proposed for a VLC system [16] which can improve cell-edge UE's performance and average spectral efficiency. In [17], the concept of multi-point joint transmission adapted to a multibeam VLC cellular network was proposed to reduce CCI and increase SINR. The main disadvantage of the approach is the requirement of synchronization among neighbor APs for cooperation. In order to minimize CCI of multibeam VLC systems, a beam selection algorithm was proposed in [18] to eliminate CCI between beams of the same VLC-AP and neighbor VLC-APs. Nevertheless, the algorithm was designed for VLC-APs which have only one active beam in each VLC-AP at any transmission time thus it might cause high packet delay and low user throughput.

Multibeam transmission is widely applied in wireless cellular mobile networks for improving the signal quality, enhancing system capacity and efficient resource utilization [19]. However, because indoor VLC networks have very small communication coverage and the design of VLC-APs has constraints of LED's parameters and installation, network configuration and interference elimination in VLC networks have to consider two following issues which do not exist in wireless cellular networks. Firstly, positions

and the directional angle of LED (which are equivalent to antenna in wireless cellular networks) are depending on the LED's lighting parameters and the layout of rooms (indoor environment). Therefore, we need a new method to design lightbeam configuration of VLC networks. Secondly, because indoor VLC-APs use very small lightbeams and commercial LEDs which have narrow bandwidth [1], it is difficult to apply interference mitigation techniques of wireless cellular networks e.g. frequency reuse, multiple access control algorithms to eliminate interference in overlapped regions of VLC-APs.

In the paper, we investigate and present solutions to solve two open research problems of multibeam multi-AP VLC systems. The first contribution of this paper is the beam configuration method aiming to provide seamless communications and minimum overlapping areas. Furthermore, the second contribution is the interference elimination resource scheduling (IERS) mechanism which includes a beam assignment algorithm and a spectrum allocation algorithm to eliminate CCI effects and enhance system performance. The remainder of the paper is organized as follows. The system model is described in Section 2. Section 3 presents the proposed lightbeam configuration method. The proposed interference aware resource scheduling (IERS) mechanism is described in Section 4. Section 5 presents the simulation results and discussions. Finally, the conclusions are given in the last section.

2 System model

In the multibeam multi-AP VLC system, VLC-APs are located in the ceiling in an indoor square layout of L (m) \times W (m) \times H (m) as shown in Figure 1. A VLC-AP deploys many lightbeams for providing directional down-link transmission as shown in Figure 2. In the paper, we

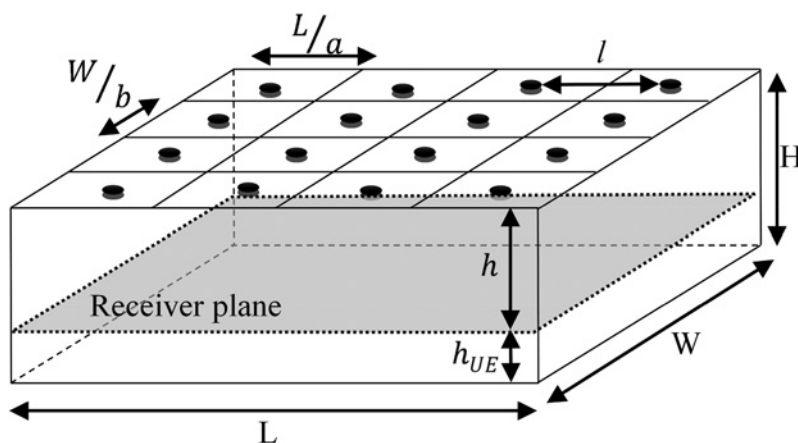


Figure 1: VLC system model: the layout of AP's location.

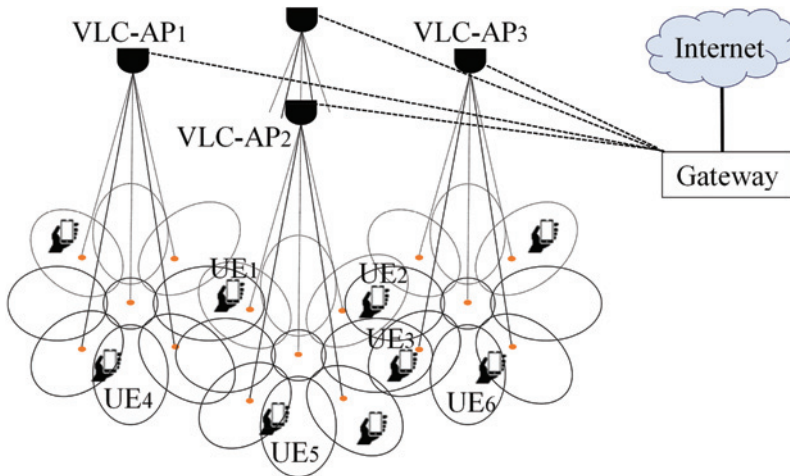


Figure 2: VLC system model: multibeam VLC-APs.

consider that the uplink channel of the VLC system can be RF or IR [20, 21]. The main components of VLC networks include gateway, VLC-AP and UE. VLC-APs connect to the Internet via the gateway. In the paper, we consider stationary UEs which are relevant to VLC systems deployed in conference rooms, offices etc.

In the multibeam multi-AP VLC system, a multibeam VLC-AP deploys a flexible multi-element transmitter to carry out optical SDMA. In the multi-element transmitter design given in [11], the number of electronically controlled elements is equal to the number of beams. In our model, the number of electronically controlled elements is less than the number of beams but each element can be flexibly connected to several beams at a given time. All LEDs of VLC-APs are always used for lighting the room. When a VLC-AP transmits data to an UE in a beam, at the physical layer, orthogonal frequency division multiplexing (OFDM) is used for the downlink channel of the beam to combat inter-symbol interference (ISI) and maximize spectral efficiency [16]. To guarantee good illumination, some signal processing techniques can be applied, for example combining the high rate OFDM communication signal with the slow rate PWM dimming signal was proposed in [22].

2.1 Downlink transmission model

Figure 3 shows that LEDs generate directional narrow field-of-view (FOV) beams with separate coverage areas. Each access point deploys a multi-element transmitter which has N_t OFDM elements ($N_t \geq 1$). The available bandwidth of each OFDM element has N_{sc} sub-channels divided into N_{RU} resource units (RU) of n_{sc} sub-channels.

A TC is defined as a dynamic group of physical beams which are electronically controlled by an OFDM

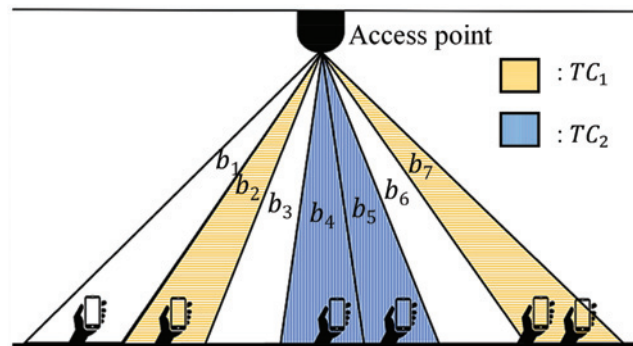


Figure 3: Downlink transmission model.

element. As illustrated in Figure 3, the AP has two OFDM elements ($N_t = 2$) corresponding to two TCs (TC_1, TC_2). Before transmitting data in a downlink time frame of the AP, the gateway selects beams and UEs located in the beams to TC_1 and TC_2 to receive data in the time frame. For example, TC_1 is assigned beams b_2 and b_7 and TC_2 is assigned beams b_4 and b_5 . UEs served by a TC share the same OFDM spectrum but each UE is allocated a certain number of RUs during allocated time slots. As the beams b_1, b_3 and b_6 are not assigned to any TC, they only perform illumination.

There are two types of downlink channels in VLC system: Line-of-sight (LOS) (from LED to UE directly) and Non-line-of-sight (NLOS) (due to the reflection of the floor, ceiling and walls) as shown in Figure 4. By using high directional beams and narrow half-intensity radiance angle of beams, the signal power received from NLOS paths is much lower than that of LOS paths. Besides, after generating the OFDM symbol, a cyclic prefix (CP) is added as a guard interval to avoid multipath induced ISI [16, 23]. Therefore, we can ignore NLOS paths and an optical channel can be accurately approximated

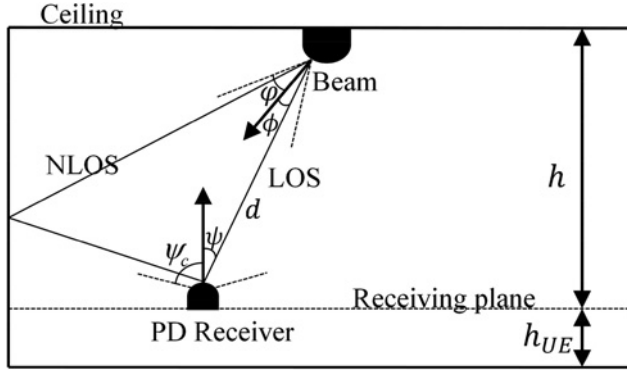


Figure 4: VLC downlink channel models.

by the LOS path. The channel DC gain is expressed as described in [24]:

$$G = \begin{cases} \frac{(m+1)A}{2\pi d^2} \cos^m(\phi) T_s(\psi) g(\psi) \cos(\psi), & 0 \leq \psi \leq \psi_c \\ 0, & \psi > \psi_c \end{cases} \quad (1)$$

where A is the physical area of the detector in Photo Detector (PD); d is the distance between the light source and the detector in PD; ψ is the incidence angle at receiver; ϕ is the angle of irradiance; $T_s(\psi)$ is the gain of an optical filter used; $g(\psi)$ is the gain of an optical concentrator; m is the Lambertian emission order given by $-\ln(2)/\ln(\cos(\varphi))$, φ is the half-intensity radiance angle of beam or LED chip and ψ_c denotes the width of the FOV at the receiver.

2.2 SINR and CCI

Because VLC-APs utilize the same OFDM spectrum bandwidth, overlapped beams belonging to different TCs of the same AP cause intra-cell interference whereas overlapped beams of different APs cause inter-cell interference. For example, as shown in Figure 2, UE_1 , UE_2 and UE_3 are affected by inter-cell interference due to residing in the overlapped region of different APs. UE_4 , UE_5 and UE_6 are affected by intra-cell interference due to being in the overlapped region of beams in the same AP.

The SINR is used to evaluate the received signal quality of UEs. Consider a UE u which is receiving the optical signal from a TC which has a set H of beams (i.e. UE u might reside in the overlapped region of set H). Assume that UE u has intra-cell CCI from a set P of beams of the same AP. Assume that UE u has inter-cell CCI from a set Q of beams belonging to neighbor APs. The received $SINR_k(u)$ of UE u on sub-channel k^{th} is expressed as:

$$\begin{aligned} SINR_k(u) &= \frac{\sum_{v \in H} (P_k R_F R_{pd} G_{u,v})^2 F_{OE}}{\sum_{v' \in P} (P_k R_F R_{pd} G_{u,v'})^2 F_{OE} + \sum_{z \in Q} (P_k R_F R_{pd} G_{u,z})^2 F_{OE} + N} \end{aligned} \quad (2)$$

where P_k is the optical transmit signal power used on sub-channel k^{th} .

$\sum_{v' \in P} (P_k R_F R_{pd} G_{u,v'})^2 F_{OE}$ is the intra-cell CCI power received from beams of the set P .

$\sum_{z \in Q} (P_k R_F R_{pd} G_{u,z})^2 F_{OE}$ is the inter-cell CCI power received from beams of the set Q .

The noise power N is defined by [16]:

$$N = 2qI_{bg}B_{sc} + \frac{4K_B T B_{sc}}{R_F} \quad (3)$$

where I_{bg} is the background current caused by the background light; B_{sc} is the bandwidth of channels allocated to user u ; the electronic charge is $q = 1.6 \times 10^{-19}$ C; K_B is the Boltzmann constant; T is the absolute temperature.

3 Lightbeam configuration method for multi-beam multi-AP VLC systems

The objective multibeam multi-AP VLC systems has the layout of AP's locations as shown in Figure 1 and deploy multibeam APs as shown in Figure 2. When configuring a VLC system for a particular indoor area which has the size of $L(m) \times W(m) \times H(m)$, we have to calculate the number of APs for fully covering the area. Because the system uses multibeam APs, we need a method to configure parameters of beams in order to have full coverage areas. Beam configuration has to fulfill two coverage requirements described below:

- Beams of an AP provide full coverage of the AP i.e. there are not blind spots between beams of the AP and overlapped areas between two beams are minimum.
- APs provide full coverage of the indoor area i.e. there are not blind spots between APs and overlapped regions between two APs are minimum.

The beam configuration method performs two calculation procedures for (1) Configuring parameters of AP's beam

layout; and (2) Configuring the number and location of APs on the ceiling.

3.1 Configuring parameters of AP's lightbeam

Configuring AP's beams has been studied in some previous researches [9, 11] where authors designed layouts of AP's beams. In [9], the author analysis performance of one-round layout (7 beams) and two-round layout (19 beams). In [11], authors also proposed layouts of the one-round layout (7 beams) and the two-round layout (19 beams) to remove blink spots. However, the previous studies did not present how to configure beam's parameters for solving two coverage requirements mentioned above.

In this section, we present a beam configuration method for designing one-round and two-round layouts of AP's beams which satisfy the two coverage requirements. Denote S_7 and S_9 are one-round layouts of 7 beams and 9 beams, respectively. Denote S_{19} and S_{25} are two-round layouts of 19 beams and 25 beams, respectively. In order to guarantee good illumination, the proposed beam configuration method uses half-intensity radiance angles of beams when calculating the VLC-AP's communications coverage. Therefore, a lighting area of LEDs of a VLC-AP is also the communication coverage i. e. satisfying both lighting and communications coverage purposes.

3.1.1 One-round beam layout configuration

The one-round configuration S_9 is illustrated in Figure 5 where φ_0 and φ_1 are the LED's standard half-intensity

radiance angle of the center beam and a first-round beam, respectively. The number of beams (N_B) is 9. The number of first-round beams (N_f) is 8. For the one-round layout design, we need to calculate the directional angle θ_1 of first round beams.

Figure 6 illustrates the coverage of the center beam and two neighbor first-round beams. The point A is the location of the AP in the ceiling. The coverage area of the center beam in the receiver plane is determined by center point O and radius R. The center of a first-round beam is denoted by P. M and N are the intersection points of these first-round beams. h is the distance between APs and the

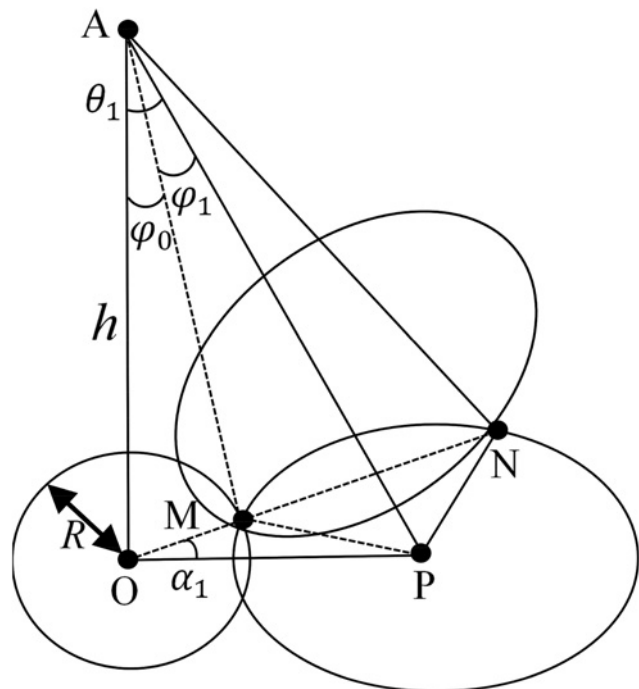


Figure 6: The one-round layout design.

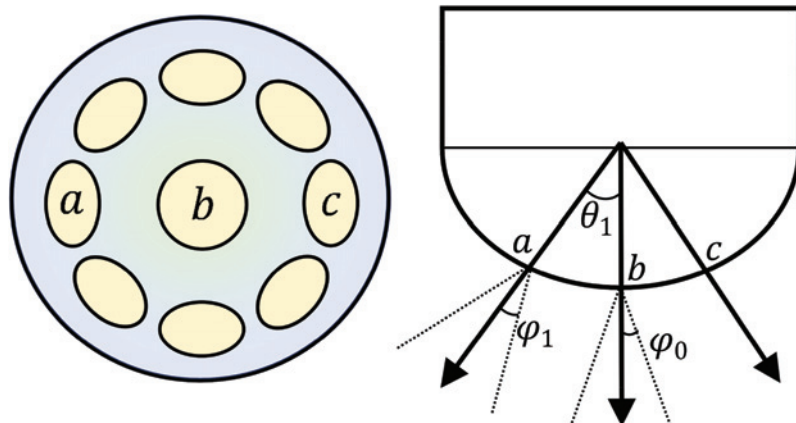


Figure 5: One-round beam layout configuration.

receiver (UE) plane. Denote α_1 is the angle of the NOP triangle which is formed by the ray OP and the ray OMN. Clearly, we have $\alpha_1 = \pi/N_1$.

To ensure that there are no blind spots in the coverage of an AP, the following condition has to be satisfied:

$$d_{OM} \leq R \quad (4)$$

Two triangles MAP and MOP have the common edge d_{MP} . Hence, d_{MP} is calculated as below:

$$\begin{aligned} d_{MP}^2 &= d_{AM}^2 + d_{AP}^2 - 2d_{AM}d_{AP} \cos \varphi_1 \\ d_{MP}^2 &= h^2 + d_{OM}^2 + h^2 + d_{OP}^2 - 2d_{AM}d_{AP} \cos \varphi_1 \end{aligned} \quad (5)$$

and,

$$d_{MP}^2 = d_{OM}^2 + d_{OP}^2 - 2d_{OM}d_{OP} \cos \alpha_1 \quad (6)$$

In which, $\angle MAP = \varphi_1$ and $\angle MOP = \alpha_1$.

From eq. (5) and eq. (6), we have:

$$d_{AM}d_{AP} \cos \varphi_1 = d_{OM}d_{OP} \cos \alpha_1 + h^2 \quad (7)$$

Considering the triangles MAO and OAP, we have following equations:

$$d_{OM} = h \tan \varphi_0, \quad d_{OP} = h \tan \theta_1$$

$$d_{AM} = \frac{h}{\cos \varphi_0}, \quad d_{AP} = \frac{h}{\cos \theta_1}$$

Replacing these distances into the eq. (7), we have:

$$\cos \varphi_1 = (\sin \varphi_0 \sin \theta_1 \cos \alpha_1) + (\cos \varphi_0 \cos \theta_1) \quad (8)$$

From (8) we determine the directional angle of first-round beams (θ_1) by the following formula:

$$\theta_1 = \pi - \arcsin \frac{\cos \varphi_0}{\sqrt{1 - \sin^2 \varphi_0 \sin^2 \alpha_1}} - \arcsin \frac{\cos \varphi_1}{\sqrt{1 - \sin^2 \varphi_0 \sin^2 \alpha_1}} \quad (9)$$

That means when designing the one-round layout of APs, the value of the directional angle of first-round beams will depend on the number of first-round beams (corresponding to the value of α_1) and the value of φ_0 and φ_1 which are LED's standard parameters. Table 1 summaries

beam configuration parameters of the layouts S_7 (06 first-round beams) and S_9 (08 first-round beams) which have $\varphi_1 = \varphi_0 = 20^\circ$.

Table 1: One-round layout parameters.

Parameters	S_7	S_9
Number of beams (N_B)	7	9
Number of the first-round beams (N_1)	6	8
Half-intensity radiance angle of the centre beam (φ_0)	20°	20°
Half-intensity radiance angle of the first-round beams (φ_1)	20°	20°
Directional angle of the first-round beams (θ_1)	34.5°	37°

3.1.2 Two-round beam layout configuration

In the two-round beam layout configuration, the number of beams in the second round doubles the number of beams in the first round $N_2 = 2N_1$ as given in [9, 11]. The two-round layout S_{25} is illustrated in Figure 7. The number of beams (N_B) is 25. The number of beams of the first-round (N_1) and second-round (N_2) are 8 and 16, respectively. φ_0 , φ_1 and φ_2 are the LED's standard half-intensity radiance angle of the center beam, first-round beams and second-round beams, respectively. For the two-round layout design, we need to calculate the directional angle θ_1 of first round beams and the directional angle θ_2 of second-round beams.

The directional angle θ_1 of first-round beams is calculated by using eq. 9. In this section, we will present how to calculate the directional angle θ_2 of second-round beams.

Figure 8 illustrates the coverage of the center beam, two neighbor first-round beams and two neighbor second-round beams. Several intersection points are denoted as below. M and N are intersection points of two first-round beams. K and L are intersection points of two second-round beams. Q is the center of a second-round beam. Denote α_2 is the angle $\angle QOL$ which is formed by the ray OL and the ray OQ. Since the number of beams in the second round is double the number of beams in the first round, then we have $\alpha_2 = \alpha_1/2 = \pi/2N_1$.

Consider two triangles NAP and NOP, we have:

$$\begin{aligned} d_{NP}^2 &= d_{AP}^2 + d_{AN}^2 - 2d_{AP}d_{AN} \cos \varphi_1 \\ d_{NP}^2 &= h^2 + d_{OP}^2 + h^2 + d_{ON}^2 - 2d_{AP}d_{AN} \cos \varphi_1 \end{aligned} \quad (10)$$

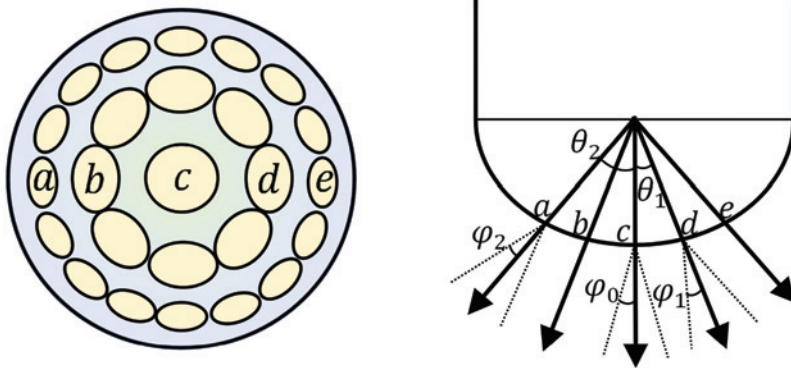


Figure 7: Two-rounds beam configurations.

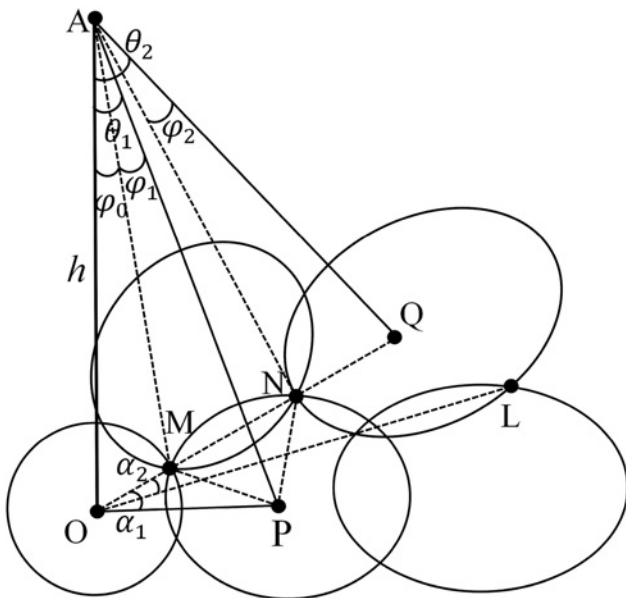


Figure 8: The two-round layout design.

and,

$$d_{NP}^2 = d_{ON}^2 + d_{OP}^2 - 2d_{ON}d_{OP} \cos \alpha_1 \quad (11)$$

In which, $\angle NAP = \varphi_1$ and $\angle MOP = \alpha_1$.

From eq. (10) and eq. (11), we have:

$$h^2 + d_{ON}d_{OP} \cos \alpha_1 = d_{AP}d_{AN} \cos \varphi_1 \quad (12)$$

Considering the triangles NAO and OAP, easily to get:

$$d_{OP} = h \tan \theta_1; d_{AP} = \frac{h}{\cos \theta_1}; d_{AN} = \sqrt{h^2 + d_{ON}^2}$$

The eq. (12) is rewritten as:

$$h^2 + d_{ON}h \tan \theta_1 \cos \alpha_1 = \frac{h}{\cos \theta_1} \times \sqrt{h^2 + d_{ON}^2} \times \cos \varphi_1 \quad (13)$$

From eqs. (13), the distances d_{ON} is calculated by:

$$d_{ON} = h \times \frac{\cos \varphi_1 \sqrt{\sin^2 \varphi_1 - \sin^2 \theta_1 \sin^2 \alpha_1} + \sin \theta_1 \cos \theta_1 \cos \alpha_1}{\cos^2 \varphi_1 - \sin^2 \theta_1 \sin^2 \alpha_1} \quad (14)$$

We have the direction-angle of second-round beam $\theta_2 = \angle OAQ$, and the half-intensity radiance angle of second-round beams φ_2 . To ensure that there are no blind spots in the two-round layout, the following condition has to be satisfied:

$$\theta_2 \leq (\angle OAN + \varphi_2) \quad (15)$$

That means the minimum overlapped area between first-round and second-round beams is determined when $\theta_2 = (\angle OAN + \varphi_2)$. Therefore, $d_{ON} = h \times \tan (\theta_2 - \varphi_2)$. So, we have:

$$\theta_2 = \arctan \left(\frac{\cos \varphi_1 \sqrt{\sin^2 \varphi_1 - \sin^2 \theta_1 \sin^2 \alpha_1} + \sin \theta_1 \cos \theta_1 \cos \alpha_1}{\cos^2 \varphi_1 - \sin^2 \theta_1 \sin^2 \alpha_1} \right) + \varphi_2 \quad (16)$$

Table 2 summaries beam configuration parameters of the layouts S_{19} and S_{25} where $\varphi_0 = \varphi_1 = 15^\circ$ and $\varphi_2 = 10^\circ$.

Table 2: Two-round layout parameters.

Parameters	S_{19}	S_{25}
Number of beams (N_B)	19	25
Number of the first-round beams (N_1)	6	8
Number of the second-round beams (N_2)	12	16
Half-intensity radiance angle of the centre beam (φ_0)	15°	15°
Half-intensity radiance angle of the first-round beams (φ_1)	15°	15°
Half-intensity radiance angle of the second-round beams (φ_2)	10°	10°
Directional angle of the first-round beams (θ_1)	26°	27.5°
Directional angle of the second-round beams (θ_2)	41°	46.5°

3.2 Configuring the number and location of APs on the ceiling

APs can be aligned on the ceiling in several forms such as Poisson Point Process, Hard-core Point Process, Hexagon and Square [25, 26]. As illustrated in Figure 1, we choose the square layout of APs for the VLC systems because the square layout is the most popular and easy implementation of lighting systems. When configuring the number of APs and their location according to size of the VLC indoor area, we have to calculate the necessary distance (l) between two adjacent APs. For a value of l and the size $L(m) \times W(m) \times H(m)$, the value of a and b , which are the necessary number of columns and rows of APs on the ceiling, are calculated:

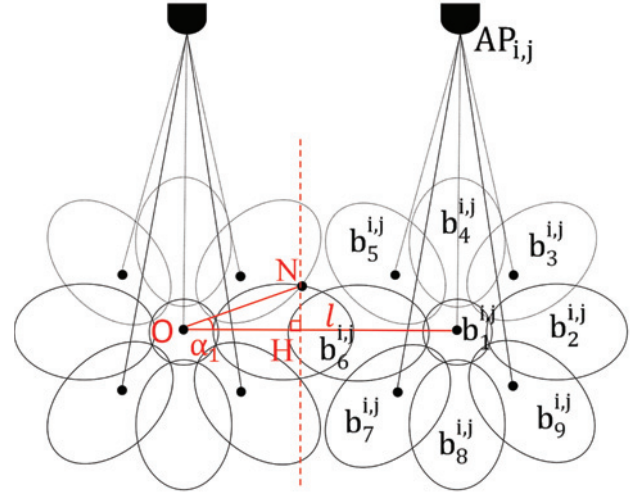
$$\begin{cases} a \geq \frac{L}{l} \\ b \geq \frac{W}{l} \end{cases} \quad (17)$$

Figure 9 illustrates the coverage of two adjacent APs when the VLC system use two multi-beam AP layouts. In order to guarantee no blind areas in the coverage of APs, we have following conditions:

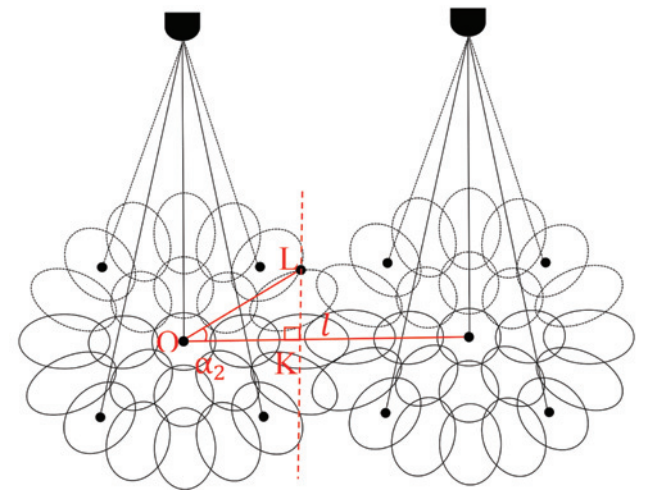
- For VLC systems which have APs using the one-round beam layout, the distance l between two adjacent APs has to satisfy:

$$\begin{aligned} l &\leq 2d_{OH} \\ l &\leq 2d_{ON} \cos \alpha_1 \\ l &\leq 2h \cos \alpha_1 \times \frac{\cos \varphi_1 \sqrt{\sin^2 \varphi_1 - \sin^2 \theta_1 \sin^2 \alpha_1} + \sin \theta_1 \cos \theta_1 \cos \alpha_1}{\cos^2 \varphi_1 - \sin^2 \theta_1 \sin^2 \alpha_1} \end{aligned} \quad (18)$$

- For VLC systems which have APs using the two-round beam layout, the distance l between two adjacent APs has to satisfy:



a) The one-round layout design



b) The two-round layout design

Figure 9: The overage area of two adjacent APs.

$$l \leq 2d_{OK}$$

$$l \leq 2d_{OL} \cos 3\alpha_2$$

d_{OL} is calculated similarly to formula (14), we have:

$$\begin{aligned} l &\leq 2h \cos 3\alpha_2 \\ &\times \frac{\cos \varphi_2 \sqrt{\sin^2 \varphi_2 - \sin^2 \theta_2 \sin^2 \alpha_2} + \sin \theta_2 \cos \theta_2 \cos \alpha_2}{\cos^2 \varphi_2 - \sin^2 \theta_2 \sin^2 \alpha_2} \end{aligned} \quad (19)$$

Table 3 shows the installation parameters to ensure there is no introduce blind area between the APs which are

Table 3: AP's installation parameters.

VLC scenarios	Conditions
S_7	$a \geq L/1.58 h, b \geq W/1.58 h$
S_9	$a \geq L/2.20 h, b \geq W/2.20 h$
S_{19}	$a \geq L/1.28 h, b \geq W/1.28 h$
S_{25}	$a \geq L/2.14 h, b \geq W/2.14 h$

calculated by using eqs. 17, 18 and 19 and layout parameters provided in Tables 1 and 2.

4 IERS mechanism

In the system model presented in Section 2, each AP has N_t OFDM elements which serve different TCs. A TC is a dynamic set of beams which are selected by the gateway before each transmission frame. If a TC has more beams, the TC will cause more interference to other TCs. Therefore, each TC will be assigned a maximum number M of beams. Before transmitting downlink data in the next time frame, the resource scheduling mechanism has to perform two functions:

- Beam assignment algorithm: Assign beams of each AP to TCs of the AP. Each TC is served by a separated OFDM element of the AP.
- Spectrum allocation algorithm: Allocate sub-channels of each OFDM element to UEs who reside in the corresponding TC.

In this section, we present our proposed IERS mechanism which includes a beam assignment algorithm implemented at the gateway and a spectrum allocation algorithm implemented at APs. First, the gateway performs the beam assignment algorithm. After the gateway completes the beam assignment, it sends to each AP a list of assigned beams of TCs of the AP. Then, the AP performs the spectrum allocation algorithm to allocate RUs to UEs served by TCs of the AP. The IERS mechanism aims to achieve following objectives:

- Eliminating intra-cell and inter-cell CCI between beams for ensuring high UE's SINR.
- Improving system performance including high throughput and low packet delay.

In order to eliminate CCI between beams, the gateway maintains a dynamic database of CCI-effect records and performs the beam assignment algorithm based on the information of the database. The dynamic

database of CCI-effect records is created and updated as described below.

4.1 Updating dynamic database of CCI-effect records

Considering the square layout of APs as shown in Figure 1, the set of APs in room is described as:

$$AP_s = \{AP_{i,j}, i \in \{1, \dots, b\}, j \in \{1, \dots, a\}\} \quad (20)$$

Thus, the AP matrix is described as:

$$AP_{a \times b} = \begin{bmatrix} AP_{1,1} & \cdots & AP_{1,a} \\ \vdots & \ddots & \vdots \\ AP_{b,1} & \cdots & AP_{b,a} \end{bmatrix} \quad (21)$$

Each $AP_{i,j}$ has N_b beams with one center beam and other beams in the first and second rounds. A beam is described as:

$$Beams = \{b_x^{i,j}, x \in \{1, \dots, N_b\}\} \quad (22)$$

The gateway maintains the database of CCI-effect records of all beams in the VLC system. An AP has an access point identifier (AP-ID). A beam of the AP has a unique beam identifier (B-ID). Each beam $b_x^{i,j}$ has a CCI record consisting the list of beams which cause intra-cell and inter-cell CCI to $b_x^{i,j}$. The CCI record has following format:

	List of B-ID of beams causing intra-cell CCI effect to $b_x^{i,j}$	List of pairs {AP-ID, B-ID} of beams causing inter-cell CCI effect to $b_x^{i,j}$
$b_x^{i,j}$		

In our previous research [18], we consider that a beam A causes CCI to a neighbor beam B regardless if there are UEs residing in their overlapped region. It means the static CCI-effect record of beam B always keeps beam A in the list of beams causing CCI-effect. Consider the case that two UEs reside in two neighbor beams but do not reside in their overlapped region. If we deploy the static CCI-effect records, one of these UEs will not be served although their transmissions do not cause CCI to each other. That can reduce the overall system performance. In the paper, the VLC system maintains and deploy a dynamic database of CCI-effect records as following:

- Periodically, an AP scans and broadcasts the B-ID of beams and also AP-ID in sub-timeslots.

- When a UE residing in the overlapped region of two or more beams, these beams can cause CCI-effect to each other. The UE receives more than one B-ID and sends the list of received B-IDs to the AP. The AP then sends the list to the gateway to update the database of CCI-effect records.

For example, consider a UE u_k which receives the B-ID of two beams $b_x^{n,m}$ and $b_y^{u,v}$. Then u_k sends the B-ID list to its AP and then the AP sends it to the gateway. The gateway determines that these beam $b_y^{u,v}$ and $b_x^{n,m}$ cause CCI to each other. The gateway updates the database i.e. if $AP_{u,v}$ is different $AP_{n,m}$ then, the B-ID of $b_x^{n,m}$ is added to the list of inter-cell CCI beams of $b_y^{u,v}$ and vice versa. If $AP_{u,v}$ is $AP_{n,m}$ then the B-ID of $b_x^{n,m}$ is added to the list of intra-cell CCI beams of $b_y^{u,v}$ and vice versa.

As mentioned in Section 2, the VLC system only has stationary UEs. Therefore, the updating period of the dynamic database of CCI-effect records is not frequent i.e. it does not cause high signaling load to the VLC system.

4.2 Lightbeam assignment algorithm

Define an active beam is the beam which has data to send to a set L of UEs. A beam has the beam priority is calculated by the formula:

$$P_b = \frac{Q_b(t)}{\bar{R}_b(t)} \quad (23)$$

where, $Q_b(t) = \sum_{u \in L} Q_u(t)$ is the total number of packets on the queue of all UEs being served by the beam at time frame t . $\bar{R}_b(t) = \frac{\sum_{u \in L} R_u(t)}{N_L}$ is the average data rate of UEs in set L at time frame t . N_L is number of UEs in the beam. $R_u(t)$ is the average data rate of UE u at time frame t .

APs calculate and send the priority P_b of all active beams to the gateway. The gateway will maintain the list L_{ab} of all active beams of the VLC system.

The gateway performs the beam assignment algorithm as follows:

4.2.1 Initiation step

A TC has a list of assigned active beams which has up to M beams. Reset the list of assigned active beams of all TCs of APs to empty.

Step 1: Sort the list L_{ab} in descending order of the beam priority.

Step 2: Assign the highest priority beam in the list L_{ab} to a TC and eliminate its intra-cell CCI beams.

Select the first beam $b_x^{i,j}$ in L_{ab} which has the highest priority and belongs to $AP_{i,j}$. Check the CCI-effect record of $b_x^{i,j}$ and the lists of assigned active beams of all TCs of the $AP_{i,j}$, following cases are considered:

- $b_x^{i,j}$ causes intra-cell CCI to more than one TCs, cancel the assignment of $b_x^{i,j}$.
- $b_x^{i,j}$ causes intra-cell CCI to only one TC_k: assign it to TC_k if the list of assigned active beams of TC_k is not full otherwise cancel the assignment of $b_x^{i,j}$.
- $b_x^{i,j}$ does not cause intra-cell CCI to any TC: assign it to TC_k which has lowest downlink load and the list of assigned active beams of TC_k is not full (the number of assigned beams is less than M). If the lists of assigned active beams of all TCs are full, cancel the assignment of beam $b_x^{i,j}$.

Step 3: Eliminate inter-cell CCI of beam $b_x^{i,j}$.

- If beam $b_x^{i,j}$ is selected for data transmission, the gateway removes all beams from the list L_{ab} which have B-ID stored in the inter-cell CCI list of its CCI record.
- Remove beam $b_x^{i,j}$ from the list L_{ab} .
- If the list L_{ab} is empty, finish the beam assignment algorithm. Otherwise, repeat Step 1.

After completing the beam assignment algorithm, the gateway sends to each $AP_{i,j}$ the list of assigned beams to corresponding TCs i.e. $\text{set}\{\text{TC}, \text{B-IDs}\}$.

4.3 Spectrum allocation algorithm

After an AP receives the list of assigned beams to corresponding TCs, the AP performs the spectrum allocation algorithm to UEs residing in each TC which is served by an OFDM element. Assume that an OFDM element has K RU. The goal of the spectrum allocation algorithm is to provide low packet delay and high user throughput.

For each OFDM element, the AP maintains a list of UEs (L_{ue}) that are being served by active beams of the corresponding TC. Each UE u has the UE priority defined as follows:

$$P_u = \frac{Q_u(t)}{R_u(t)} \quad (24)$$

where, $Q_u(t)$ is the total number of packets on the UE u waiting in the downlink queue at time frame t ; $R_u(t)$ is the average data rate of UE u at time frame t .

The spectrum allocation algorithm is described as follows:

Step 1: Sort L_{ue} in descending order of the UE priority.

Step 2: Consider the first UE named u_x in the list L_{ue} (i.e. u_x has the highest priority) and do the RU allocation as following:

- Allocate 1 RU to UE u_x . Calculate the number of packets of UE u_x which will be delivered in the next time frame by using the RU:

$$Packet_number = \frac{timeFrame_duration \times R_{ru}}{Packet_size} \quad (25)$$

where, $Packet_number$ is the number of data packets of UE u_x to be sent by using the RU in the next timeframe; R_{ru} is the data rate allocated to UE u_x using the RU.

- Update the remaining packets Q_{u_x} on the queue:

$$Q_{u_x}(t) = Q_{u_x}(t) - Packet_number \quad (26)$$

- Update the average data rate for UE u_x by the following expression:

$$R_u(t+1) = \left(1 - \frac{1}{T_c}\right)R_u(t) + \frac{1}{T_c}R_{ru} \quad (27)$$

where, T_c is the constant number (define $T_c = 1000$); $R_u(t)$ is the average data rate of UE u_x at time t .

- Update the UE priority P_u of UE u_x .
- If L_{ue} is empty or all RUs have been allocated then go to Step 3. Otherwise, repeat Step 1.

Step 3: Continue to do spectrum allocation algorithm for other TCs until all TCs finish the spectrum allocation.

For all other UEs of the AP which have not been selected for transmitting in the next time frame, the AP updates their average rate with $R_{ru} = 0$.

5 Results and discussions

The simulation layout has dimensions of 16 m × 16 m × 3 m. The height h of UE's PD receiver is 1 m. The FOV of UE's PD receivers is directed towards the ceiling and

perpendicular to the UE plane. UEs are uniformly distributed in the simulation area. New connections are generated following the Poisson process with the mean arrival rate of five (05) connections/minute for each AP. The connection duration is exponentially distributed with the mean duration of 180 seconds. Downlink traffic of each UE is generated in a Poisson process which has packet size of 10.8 kbits and the mean inter-arrival duration of 1.5 milliseconds (the average load of an AP is about 80%, estimate). The VLC downlink channel is assumed to be flat and invariant over time.

The simulated VLC system deploys four lightbeam layouts S_7 , S_9 , S_{19} and S_{25} . Using Table 3, we calculate the number of APs and the locations of APs in the square layout (Figure 1) as given in Table 4.

Table 4: AP's layout configuration.

Configuration	Installation parameter	Number of APs
S_7	$a \geq 5, b \geq 5$	5×5
S_9	$a \geq 3.6, b \geq 3.6$	4×4
S_{19}	$a \geq 6.3, b \geq 6.3$	7×7
S_{25}	$a \geq 3.7, b \geq 3.7$	4×4

When drawing the coverage of APs using Matlab, we observe that S_7 and S_9 lightbeam layouts have large blind spots between lightbeam's footprint. Therefore, with a given room dimensions, in order to provide full coverage, the number of APs needed when using S_7 and S_{19} lightbeam layouts is higher than when using S_9 and S_{25} lightbeam layouts (S_7 requires 25 APs and S_{19} requires 49 APs while S_9 and S_{25} requires only 16 APs). Using S_9 and S_{25} lightbeam layouts reduces the size of overlapped areas between APs, i.e., reducing CCI-effect areas. The overlapped area between APs is very large when deploying S_7 and S_{19} lightbeam layouts i.e. large CCI-effect areas. That conclusion will be proved by simulation results in the Sub-Section 5.2.

The simulation parameters of the VLC system which are taken from [17] are presented in Table 5.

5.1 Performance comparison of the proposed IERS and Round-Robin scheduling

In this section, we evaluate and compare the performance of the IERS with those of the popular Round-Robin (RR) scheduling which is applied for both lightbeam assignment and spectrum allocation algorithms.

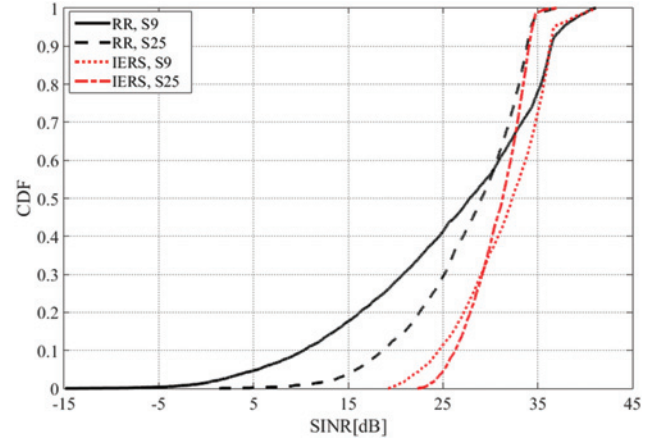
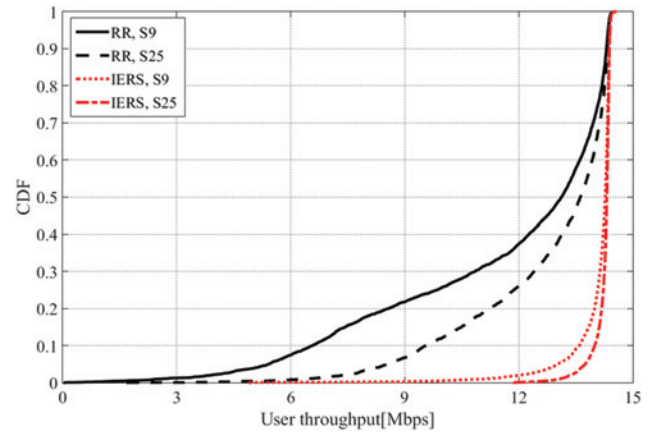
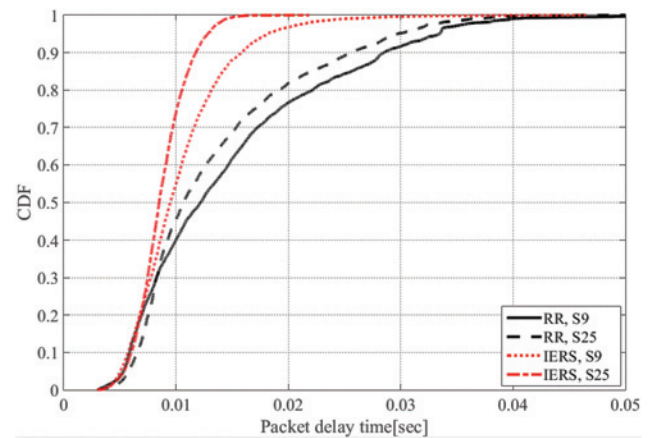
Table 5: Simulation parameters of the VLC system.

Parameters	Unit	Value
Simulation time (T)	Seconds	3600
Time slot duration (T_s)	Seconds	0.001
Frame Size (T_F)	Timeslot	4
AP optical power (P_{AP})	W	34
PD responsivity (R_{pd})	A/W	0.28
PD physical area (A)	cm ²	1.5
Receiver field of view (ψ_c)	Degree	70 ^o
Current due to background light (I_{bg})	μ A	5100
Feedback resistance of TIA (R_F)	k Ω	6
E/O conversion factor (F_{OE})		1/9
System bandwidth (B)	MHz	20
Thresholds SINR ($SINR_{th}$) for 64-QAM OFDM	dB	16.6
Number of RUs each AP (N_{RU})	RU	10
Packet size (p)	Kbits	10.8
Number of OFDM elements in an AP (N_c)		2
Maximum number of lightbeams being assigned to each transmission cluster		2

We choose RR scheduling for performance comparison because it can provide fair resource scheduling to UEs and is also applied in wireless communications systems. In other similar research on multibeam VLC networks, RR scheduling has been used in [11] to allocate time slots to users in lightbeams. To our best knowledge, there are not beam scheduling mechanisms proposed for multi-beam multi-AP VLC networks. Therefore, in the scope of the paper, we carry out the performance comparison of IERS and RR scheduling in order to show the effectiveness of the proposed IERS. Performance metric includes receiver SINR, user throughput and packet delay. The deployment of the RR scheduling mechanism is as follows:

- RR lightbeam assignment algorithm: for each AP, the gateway selects and assigns active beams to the AP's OFDM elements in the round-robin operation until the lists of assigned active beams of all TCs are full.
- RR spectrum allocation algorithm: An AP allocates RUs to UEs residing in each TC in the round-robin operation.

In the first simulation experiment, the VLC system deploys S_9 and S_{25} lightbeam layouts. Performance results are presented as the cumulative distribution function (CDF) of UE's SINR, user throughput and packet delay as presented in Figures 10, 11 and 12, respectively. Simulation results presented in Figure 10 prove that by using the database of CCI-effect records in the proposed IERS mechanism, intra-cell and inter-cell CCI are well eliminated resulting in much better UE's SINR. For example, when using the IERS mechanism, the percentage of

**Figure 10:** SINR evaluation and comparison.**Figure 11:** Throughput evaluation and comparison.**Figure 12:** Packet delay evaluation and comparison.

SINR samples higher than 19 dB is 100% whereas the value of the RR mechanism is 75% and 90% in S_9 and S_{25} , respectively. That means by applying the IERS

mechanism, all UEs have SINR higher the thresholds SINR (SINR_{th}) for 64-QAM OFDM. It also proves that using more beams in an AP, the intra-cell CCI-effect is reduced. Using S_9 (one-round model) has higher SINR than S_{25} (two-round model). For example, 30% of SINR samples using S_9 layout (IERS, S_9) is higher than 35 dB whereas using S_{25} layout (IERS, S_{25}) only has about 1% of SINR samples of 35dB. The reason is the optical power of a lightbeam of the one-round layout is higher than that of two-round layout. Therefore, UEs residing in S_9 has higher SINR than in S_{25} lightbeam layouts.

Figure 11 shows that deploying the IERS mechanism can enhance the UE's throughput significantly. The IERS mechanism provides more than 80% and 90% of throughput samples of S_9 and S_{25} lightbeam layouts higher than 14 Mbps, respectively. The percentage of throughput samples higher than 14 Mbps of the RR mechanism for S_9 and S_{25} lightbeam layouts are only 28% and 37%, respectively.

Figure 12 shows the improvement of packet delay when deploying the IERS mechanism which provides 85.5% and 99.8% delay samples smaller than 0.015s for S_9 and S_{25} lightbeam layouts, respectively. The percentage of delay samples smaller than 0.015s of the RR mechanism for S_9 and S_{25} lightbeam layouts are 60.5% and 69%, respectively.

Figures 11 and 12 show that the IERS mechanism can eliminate CCI between beams thus it can provide better performance. Performance results also prove that using the two-round model (S_{25}) achieves better throughput and packet delay than using the one-round model (S_9) because when the AP has more beams, the diversity of VLC networks is better resulting in better spectrum utilization.

5.2 Performance evaluation of the IERS mechanism deploying in different lightbeam layouts

In the simulation experiment, we evaluate and compare the VLC system performance in terms of user throughput and packet delay for VLC systems deploying different lightbeam layouts (S_7 , S_9 , S_{19} , S_{25}). Except common simulation parameters shown in Table 5, system configurations of four simulation scenarios are given in Table 6 below.

The purpose of the simulation experiment is to observe the effectiveness of the IERS mechanism in different system configuration for the same indoor space

Table 6: Sample caption.

Scenario	S_7	S_9	S_{19}	S_{25}
Lightbeam model	One-round	One-round	Two-round	Two-round
Number of AP (Table 4)	25	16	49	16
Number of OFDM element in an AP (N_i)	2	3	1	3
Total number of OFDM elements	50	48	49	48

and similar total number of OFDM elements, i.e., four scenarios have almost the same spectrum capacity.

Performance results are presented as the CDF of user throughput and packet delay as presented in Figures 13 and 14, respectively. In general, when the VLC system deploys two-round lightbeam layouts (S_{19} and S_{25}), it can provide higher user throughput and lower packet delay than those of one-round lightbeam layouts (S_7 and S_9). For example, Figure 13 shows that the percentage of throughput samples higher than 20 Mbps in scenarios S_7 , S_9 , S_{19} and S_{25} is 65%, 74%, 88% and 97%, respectively. Similarly, Figure 14 shows that the percentage of delay samples lower than 0.015s in scenarios S_7 , S_9 , S_{19} and S_{25} is 76%, 83%, 96% and 99%, respectively.

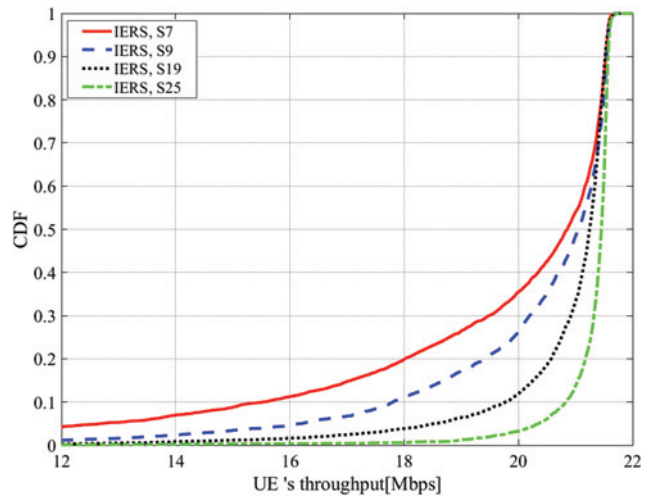


Figure 13: IERS's throughput comparison.

Therefore, when we need to select the appropriate lightbeam layouts for system configuration, we should choose S_9 for the one-round model and S_{25} for the two-round model because the performance of S_9 and S_{25} is better than that of S_7 and S_{19} , respectively whereas the number of APs of S_9 and S_{25} is much smaller than that of S_7 and S_{19} ,

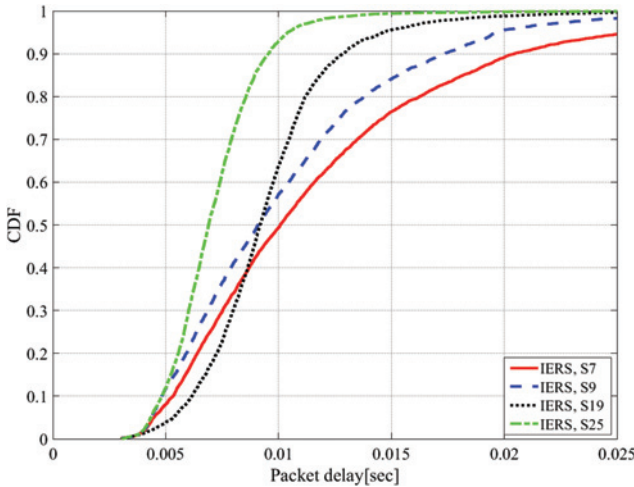


Figure 14: IERS's packet delay comparison.

respectively. This proves that by using multi-element APs, the number of required APs can be reduced but the system performance is still better than using traditional single-element APs.

5.3 Performance evaluation the IERS mechanism considering impacts of TCs

In the simulation experiment, we evaluate the VLC system performance of the IERS mechanism while considering the impacts of TCs. We use the lightbeam layout S_9 and S_{25} for configuring APs. For an AP, the number of OFDM element is 2 ($N_t=2$). We change the maximum number of lightbeams assigned to a TCs ($M=1, 2, 3$). Other simulation parameters are also given in Table 5. Performance results are presented as the CDF of user throughput and packet delay as presented in Figures 15 and 16, respectively.

Figures 15 and 16 show that if only one beam is assigned to a TC which is served by an OFDM element, the system performance is not good because the spectrum of the OFDM element might be not fully utilized. In the S_9 scenario, when more beams are assigned of a TC, performance is increased slightly because there are only 9 beams in an AP. If a TC is assigned more lightbeams, it will cause more interference to other beams. For the S_{25} scenario, assigning two or three beams to a TC does not cause much different of system performance. From the simulation data, we discover that the one-round lightbeam model (S_9) should exploit one beam per one TC whereas the two-round model can exploit two or three beams per TCs.

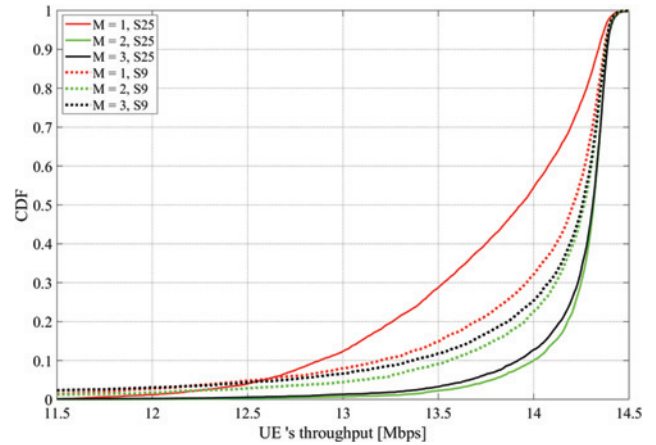


Figure 15: CDF of user throughput when using different values of M .

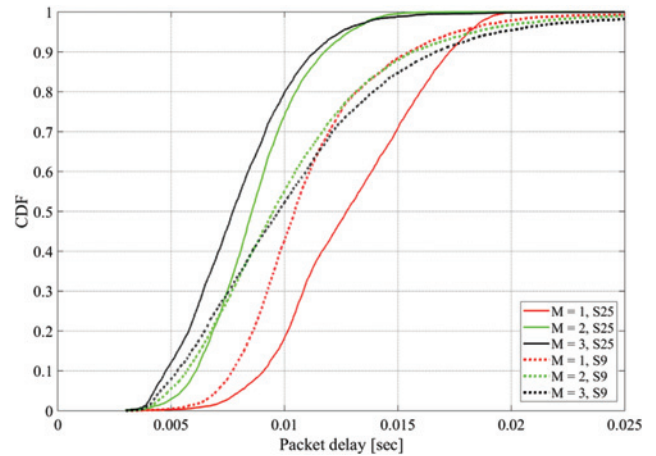


Figure 16: CDF of packet delay when using different values of M .

6 Conclusions

In the paper, we investigated and proposed solutions to solve two open research problems of multibeam multi-AP VLC systems. The first contribution is a lightbeam configuration method which provides seamless communications and minimum overlapped areas. The second contribution is the IERS mechanism which can eliminate intra-cell and inter-cell CCI and improve system performance. Simulation results proved that our lightbeam configuration method can support the system designer to select the most appropriate system configuration parameters. Performance results proved that the IERS mechanism is able to eliminate CCI and thus increase user throughput and reduce packet delay. Future works include the extension of our research to heterogeneous VLC systems which deploy different types of APs and have different user distribution and traffic types.

Acknowledgements: This work has been supported by Vietnam National University, Hanoi under Project QG.18.35 “Research on interference mitigation and performance enhancement and development of a simulation tool for beam-steering visible light communications networks”.

References

1. Medina C, Zambrano M, Navarro K. Led based visible light communication: technology, applications and challenges – a survey. *Int J Adv Eng Technol.* Aug 2015;8:482–5.
2. Sevincer A, Bhattarai A, Bilgi M, Yuksel M, Pala N. LIGHTNETS: smart lighting and mobile optical wireless networks – a survey. *IEEE Commun Surv Tut.* Apr 2013;15:1620–41.
3. Hou R, Chen Y, Wu J, Zhang H. A brief survey of optical wireless communication. *Proc Australas Symp Parallel Distrib Comput (AusPDC2015).* Jan 2015;27-30:41–50.
4. Bhalerao M, Sonavane S, Kumar V. A survey of wireless communication using visible light. *Int J Adv Eng Technol.* Jan 2013;5:188–97.
5. Karunatilaka D, Zafar F, Kalavally V, Parthiban R. LED based indoor visible light communications: state of the art. *IEEE Commun Surv Tut.* Mar 2015;17:1649–78.
6. Bui TC, Kiravittayaet S, Nguyen NH, Nguyen NT, Spirinmanwat K. Leds configuration method for supporting handover in visible light communication. *Proceedings IEEE Region 10 Conference TENCON.* 2014 Oct:1–6.
7. Kim SM, Kim SM. Performance improvement of visible light communications using optical beamforming. *2013 Fifth International Conference on Ubiquitous and Future Networks (ICUFN).* 2013: 362–5.
8. Kim SM, Lee HJ. Visible light communication based on space-division multiple access optical beamforming. *Chin Opt Lett.* 2014;12:120601.
9. Eroglu YS, Sahin A, Guvenc I, Pala N, Yuksel M. MultiElement transmitter design and performance evaluation for visible light communication. *2015 IEEE Globecom Workshops (GC Wkshps).* San Diego CA, 2015 Dec: 1–6.
10. Mushfique SI, Palathingal P, Eroglu YS, Yuksel M, Guvenc I, Pala N. A software-defined multi-element VLC architecture. *IEEE Commun Mag.* Feb 2018;56:196–203.
11. Chen Z, Basnayaka DA, Haas H. Space division multiple access for optical attocell network using angle diversity transmitters. *IEEE J Lightw Technol.* Jun 2017;35:2118–31.
12. Yin L, Haas H. Physical-layer security in multiuser visible light communication networks. *IEEE J Sel Areas Commun.* Jan 2018;36:162–74.
13. Marsh GW, Kahn JM. Channel reuse strategies for indoor infrared wireless communications. *IEEE Trans Commun.* Oct 1997;45:1280–90.
14. Cui K, Quan J, Xu Z. Performance of indoor optical femtocell by visible light communication. *Opt Commun.* Jul 2013;298/299:59–66.
15. Chen C, Videv S, Tsonev D, Haas H. Fractional frequency reuse in DCO-OFDM based optical attocell networks. *J Lightwave Technol.* Oct 2015;33:3986–4000.
16. Ghimire B, Haas H. Self-organising interference coordination in optical wireless networks. *EURASIP J Wirel Commun Netw.* 2012;2012:1–15.
17. Chen C, Tsonev D, Haas H. Joint transmission in indoor visible light communication downlink cellular networks. *2013 IEEE Globecom Workshops (GC Wkshps).* 2013 Dec: 1127–32.
18. Nguyen DQ, Nguyen NT, Nguyen NH, Spirinmanwat K. Light beam allocation algorithm for eliminating interference in visible light communications. *IEEE ATC’2016.* Hanoi. 2016 Oct: 419–25.
19. Kutty S, Sen D. Beamforming for Millimeter Wave Communications: an Inclusive Survey. *IEEE Commun Surv Tutorials.* 2016;18:949–73.
20. Langer KD, Grubor J. Recent developments in optical wireless communications using infrared and visible light. *2007 9th International Conference on Transparent Optical Networks (ICTON).* 3 Jul 2007: 146–51.
21. Shao S, Khreishah A, Rahaim MB, Elgala H, Ayyash M, Little T, et al. An indoor hybrid WIFI-VLC internet access system. *Proceedings IEEE 11th International Conference MASS.* 2014 Oct: 569–74.
22. Elgala H, Little TDC. Reverse polarity optical-OFDM (RPO-OFDM): dimming compatible OFDM for gigabit VLC links. *Opt Exp.* 2013;21:24288–99.
23. Mossaad M, Hranilovic S. Practical OFDM signalling for visible light communications using spatial summation. *2014 27th Biennial Symposium on Communications (QBSC).* Jul 2014: 5–9.
24. Komine T, Nakagawa M. Fundamental analysis for visible-light communication system using LED lights. *IEEE T Consum Electr.* Feb 2004;50:100–7.
25. Haas H, Yin L, Wang Y, Chen C. What is LiFi? *J Light Technol.* 2016;34:1533–44.
26. Chen C, Basnayaka DA, Haas H. Downlink performance of optical attocell networks. *J Lightwave Technol.* Jan 2016;34:137–56.